Pathology - Research and Practice 215 (2019) 209–214

Contents lists available at ScienceDirect

Pathology - Research and Practice

journal homepage: www.elsevier.com/locate/prp

Immune checkpoint blockade resistance-related *B2M* hotspot mutations in microsatellite-unstable colorectal carcinoma

Su Yeon Yeon[a,b,1], Seung-Hyun Jung[b,c,1], Yun Sol Jo[a], Eun Ji Choi[a], Min Sung Kim[a,b], Yeun-Jun Chung[c,d,e,**], Sug Hyung Lee[a,b,*]

[a] Departments of Pathology, College of Medicine, The Catholic University of Korea, Seoul 137-701, Republic of Korea
[b] Departments of Cancer Evolution Research Center, College of Medicine, The Catholic University of Korea, Seoul 137-701, Republic of Korea
[c] Departments of Integrated Research Center for Genome Polymorphism, College of Medicine, The Catholic University of Korea, Seoul 137-701, Republic of Korea
[d] Departments of Precision Medicine Research Center, College of Medicine, The Catholic University of Korea, Seoul 137-701, Republic of Korea
[e] Departments of Microbiology, College of Medicine, The Catholic University of Korea, Seoul 137-701, Republic of Korea

ARTICLE INFO

Keywords:
Immune checkpoint blockade
B2M mutation
Colorectal cancer
Cancer panel

ABSTRACT

β2-microglobulin (B2M), a component of major histocompatibility complex class I, plays an important role in host immune reaction to tumor, and inactivation of B2M is known to contribute to resistance to immune checkpoint blockade (ICB) treatment. To further characterize the *B2M* alterations in tumors, we analyzed *B2M* hotspot mutations in 2765 benign and malignant tumor tissues by Sanger sequencing and found *B2M* mutations in 9 (7.5%) microsatellite-unstable (MSU) colorectal cancers (CRCs) and 3 leukemias (0.6–1.3%), but not in other tumors. Targeted sequencing panel analysis for MSU CRCs showed that *B2M*-mutated MSU CRCs harbored more driver mutations including *TP53* than *B2M*-wild-type MSU CRCs. Of note, bi-allelic *B2M* alterations, which had been known to be accumulated during ICB treatment, were frequently found (3/9) in ICB treatment-naive CRCs. Clinicopathologic parameters including CD8 + T cell numbers, cancer stages and patients' survival, however, were not significantly different between *B2M*-mutated and *B2M*-wild-type MSU CRCs. Our results indicate that *B2M* mutation abundance is tissue type-specific (e.g., MSU CRCs) and that genetic makeup of *B2M* mutation might possibly shape the MSU CRC genomes even before the ICB therapies. Our results show that *B2M* mutation is common in MSU CRCs, which is one of the main targets for ICB treatment, suggesting that frequent *B2M* mutation status should be reminded for MSU CRCs in patient selection of ICB.

1. Introduction

Cancer cells often have molecules on their surface that can be detected by the immune system, known as tumor-associated antigens, which can be targeted by immunotherapies [1–4]. Among the immunotherapeutic strategies, the immune checkpoint blockade (ICB) represents a major breakthrough in cancer therapy and has successfully revealed that a subset of tumors such as melanoma and mismatch repair deficiency (dMMR) cancers are sensitive to the ICBs [5,6]. Cancer cells may use the immune checkpoints to protect themselves from host immune attacks [7], and thus ICB may increase antitumor immunity by blocking immune inhibitions, including cytotoxic T-lymphocyte antigen 4 (CTLA-4), programmed cell death 1 (PD-1) and its ligand (PD-L1) [1–4,7]. However, the ICB therapies remain ineffective in many cancers for several mechanisms. For example, somatic loss of function mutations in *B2M, JAK1* and *JAK2* as well as structural variations disrupting the *PD-L1* 3′ region have been discovered as mechanisms underlying the resistance [8,9].

Major histocompatibility complex (MHC) class I that consists of two polypeptide chains (α and β2-microglobulin (B2M)) plays a pivotal role in presenting antigens to cytotoxic T cells [10]. B2M is important in proper MHC class I folding and transport to the cell surface, and inactivation of B2M has been recognized as mechanisms for both MHC class I inactivation and resistance to immunotherapies [5,8,11–14]. Intrinsic loss of B2M expression has been identified in pre-immunotherapy samples of colorectal cancers (CRC) and melanomas

* Corresponding author at: Department of Pathology, College of Medicine, The Catholic University of Korea, 222 Banpo-daero, Socho-gu, Seoul 06591, Republic of Korea.
** Corresponding author at: Department of Microbiology, College of Medicine, The Catholic University of Korea, 222 Banpo-daero, Socho-gu, Seoul 06591, Republic of Korea.
E-mail addresses: yejun@catholic.ac.kr (Y.-J. Chung), suhulee@catholic.ac.kr (S.H. Lee).
[1] These two authors contributed equally to this work.

https://doi.org/10.1016/j.prp.2018.11.014
Received 1 October 2018; Received in revised form 7 November 2018; Accepted 23 November 2018

[14,15]. Also, B2M losses by homozygous mutation and/or *B2M* allele deletion as acquired events have been found in recurrent CRC, melanoma and lung cancer after ICB [5,8,11]. Stepwise accumulation of *B2M* alterations ('single to double mutations' or 'one allele loss to two allele losses' or 'one allele loss to one allele loss plus one allele mutation') has been addressed during the immunotherapies as well [5,11,14].

One of the main issues in cancer genetics is to address whether pathogenesis-associated or therapy-related mutation is specific to a few cancer types or a general phenomenon. In order to further characterize *B2M* mutations in human tumors, we investigated whether pre-immunotherapy cancer tissues of various histological types harbor *B2M* mutations and found that microsatellite-unstable (MSU) CRC harbored frequent *B2M* mutations in this study.

2. Material and methods

2.1. B2M gene analysis

The 2765 tissue specimens used in this study consisted of 1509 epithelial tumors, 295 mesenchymal tumors and 961 lympho-hematopoietic tumors that involved both benign and malignant tumors (Table 1). Approval was obtained from the Catholic University of Korea, College of Medicine's institutional review board for this study. Tumor cells and normal cells were selectively procured from hematoxylin and eosin-stained slides of formalin-fixed paraffin-embedded (FFPE) tissues by microdissection as described previously [16]. The previous work by Zaretsky et al. [8] identified recurrent 4 basepair deletion (TCTT) mutation of *B2M* in the exon 1 (c.del42_45, p.S16Afsx27) that would result in truncation of the B2M protein. Thus, we focused our analysis on this region of *B2M* gene by polymerase chain reaction (PCR)-based single-strand conformation polymorphism (SSCP) analysis for the mutation detection [16]. Genomic DNA each from tumor cells and normal cells was amplified by PCR with a specific primer pair (forward and reverse, respectively: 5′-CTGGCGGGCATTCCTGAAG-3′ and 5′-AGAGG GTGCAGAGCGGGAGA-3′, product size: 161 bps) and mobility shifts in the SSCP were further analyzed by Sanger sequencing as described previously [16]. For microsatellite instability status analysis, we used multiplex PCR for five quasi-monomorphic mononucleotide repeats (BAT25, BAT26, NR21, NR24, and NR27). Cancers with no allelic size variations in fewer than two of the microsatellites were considered microsatellite-stable (MSS), while those with size variations in more than two microsatellite markers were considered MSU.

2.2. Targeted deep sequencing

For the samples that were confirmed to harbor *B2M* mutations through SSCP-based Sanger sequencing, a targeted deep sequencing was performed to further characterize the genome structures of *B2M*-mutated tumors. Because *B2M* mutations were mainly found in MSU CRCs, we analyzed nine *B2M*-mutated and 10 *B2M*-non-mutated MSU CRCs by targeted next generation sequencing (NGS). Acquisition and processing of the sequencing data were performed as previously described [17]. In brief, genomic DNA from tumor and matched adjacent normal samples was subjected to target capture using the OncoChase Hybrid Cancer Panel (ConnectaGen, Korea) consisting of 119 genes (Supplementary Table 1). Targeted NGS was conducted using an Illumina HiSeq4000 platform to generate 101-bp paired-end reads. A Burrows-Wheeler aligner was used to align the sequencing reads onto the human reference genome (UCSC hg19). Point mutations and indels were identified using MuTect [18] and SomaticIndelDetector [19], respectively. The ANNOVAR package [20] was used to select somatic variants located in the exonic sequences and to predict their functional consequences. DNA copy number profiling for these 19 CRCs was estimated on the basis of read depth difference between the tumor and the normal using NEXUS software v9.0 (Biodiscovery Inc., USA).

Table 1
B2M mutations in 2765 tumors analyzed.

Type of tumors	Number of tumors	*B2M*			
		Wild type	Mutation	Mutation (%)	Mutated case (detection method*)
Adulthood AML	250	250	0	0	
Adulthood ALL	176	175	1	0.6	c.del43-44CT (S)
Childhood AML	21	21	0	0	
Childhood ALL	251	250	1	0.4	c.-4C > T (S)
Multiple myeloma	75	74	1	1.3	c.del43-44CT (S)
Myelodysplasia	68	68	0	0	
Lymphomas	120	120	0	0	
Gastric carcinoma	190	190	0	0	
MSU	34	34	0	0	
MSS	156	156	0	0	
Colorectal carcinoma	493	484	9	1.8	
MSU	120	111	9	7.5	c.del43-44CT (S, T), c.16delG (S, T), c.42_45delTCTT (T), c.67 + 2T > C (S, T), c.3 G > A (S, T)
MSS	373	0	0	0	
Breast carcinoma	81	81	0	0	
Prostate carcinoma	294	294	0	0	
Ovarian stromal tumors	100	100	0	0	
Ovarian carcinoma	23	23	0	0	
Hepatocellular carcinomas	45	45	0	0	
Hepatoblastoma	23	23	0	0	
Leiomyoma	67	67	0	0	
Adenocarcinomas, lung	100	100	0	0	
Squamous cell carcinomas, esophagus	67	67	0	0	
Squamous cell carcinomas, larynx	74	74	0	0	
Squamous cell carcinomas, lung	119	119	0	0	
Sarcomas	110	110	0	0	
Meningioma	18	18	0	0	
Total	2765	2753	12	0.43	

AML: acute myelogenous leukemia, ALL: acute lymphoblastic leukemia, MSU: microsatellite-unstable, MSS: microsatellite-stable.
* S: Sanger sequencing, T: targeted NGS sequencing.

2.3. Immunohistochemistry (IHC)

IHC for identifying CD8 + T cells was performed using 19 CRC tissues that consisted of the nine *B2M*-mutated CRCs and 10 B2M-wild-type CRCs. We used ImmPRESS System (Vector Laboratories, Burlingame, CA) with the mouse polyclonal antibody for CD8 (clone C8/144B, dilution 1:4, DakoCytomation, Glostrup, Denmark) overnight at 4 °C. The IHC procedure was performed as described previously.[16] The reaction products were developed with diaminobenzidine and counterstained with hematoxylin. After the IHC, resulting slides were examined under a microscope by two pathologists. Numbers of stained T cells were counted under 10x high power field (HPF) at 10 sites.

2.4. Statistical analysis

Statistical analyses were performed using R Statistical Software (Foundation for Statistical Computing, Vienna, Austria). Fisher's exact test was used to compare categorical variables, whereas non-parametric Wilcoxon-Mann-Whitney rank-sum test was used to compare continuous variables. *P* values less than 0.05 were considered to be statistically significant to test null hypothesis.

3. Results

3.1. B2M mutation analysis

Genomic DNAs of 2765 tumors were analyzed to detect mutations in known hotspot sites of *B2M* by PCR-SSCP analysis followed by Sanger sequencing, which revealed 14 somatic mutations in 12 cases (9 CRCs, 1 adulthood acute lymphoblastic leukemia (ALL), 1 childhood ALL and 1 multiple myeloma), but none in the other tumors (Table 1, Supplementary Fig. 1). The mutations consisted of 11 frameshift mutations and 3 substitution mutations (5′-untranslated region, splicing donor site and start codon). CRC2 and CRC6 harbored 2 mutations each, while the other 10 cases harbored one mutation each (Tables 1 and 2). Matched normal samples did not harbor the mutations. Interestingly, all of the mutations in CRCs were found only in MSU cases, but not in MSS cases.

3.2. Targeted deep sequencing

Since most of the *B2M* mutations in the Sanger sequencing analysis were found in MSU CRCs (9/12), we attempted to analyze genomic features of *B2M*-mutated MSU CRCs by comparing the 9 *B2M*-mutated and 10 *B2M*-wild-type MSU CRCs with a targeted deep sequencing panel consisting of 119 cancer-related genes. There was no significant difference in the clinocopathologic characteristics, including patients' survival between these two groups ($p > 0.05$, Fisher's exact test) (Supplementary Table 2). Median depth of coverage for the targeted deep sequencing was 619.5x (range 327x-1103x) (Supplementary Table S3). We identified 9–53 non-silent somatic mutations and indels per sample (median: 16, average: 19) (Fig. 1). All of the mutations found in the deep sequencing (Supplementary Table S4) were previously reported in CRCs (COSMIC database). Seven mutated genes (*APC*, *PIK3CA*, *TP53*, *ATM*, *FBXW7*, *ARID1A* and *BRAF*) overlapped the CRC top 20 genes in the COSMIC database (http://cancer.sanger.ac.uk/cosmic). Besides these 7 genes, we found that 10 genes were recurrently mutated in more than two CRCs (Table 2).

Of the nine CRCs with *B2M* mutations, three (CRC2, CRC6 and CRC9) harbored bi-allelic *B2M* mutations at different alleles, while the other six harbored one *B2M* mutation each (Fig. 2). A newly detected mutation of *B2M* by the targeted sequencing that had not been detected by Sanger sequencing was c.42_45delTCTT in CRC9. In the CRC9, allele frequency of this c.42_45delTCTT (0.9%) was much lower than the c.43_44delCT (9.8%) (Supplementary Fig. 2) that had been detected by Sanger sequencing. CRC2 and CRC6 harbored splicing site/frameshift mutations and substitution/frameshift mutations, respectively (Supplementary Table 4). *B2M*-mutated CRCs (average: 4.89 mutations) harbored a significantly higher number of nonsynonymous mutations than *B2M*-wild-type CRCs (2 mutations) ($P < 0.05$). In addition, *B2M*-mutated CRCs tended to harbor more frequent *TP53* mutations (4/9) and less frequent *APC* mutations (1/9) than *B2M*-wild-type CRCs (2/10 and 5/10, respectively), although there was no statistical significance ($P = 0.259$ and $P = 0.091$, respectively).

3.3. Copy number profiles

By using the targeted sequencing data, we analyzed copy number profiles of the 19 CRCs. There were somatic copy number gains on 8q for 3 CRCs (CRC5, CRC13 and CRC18), on 8p for 2 CRCs (CRC13 and CRC18) and on chromosome 12 for 2 CRCs (CRC11 and CRC17). The other 14 CRCs did not reveal any distinguished copy number alterations (CNA). There was no CNA encompassing chromosome 15q21.1 where

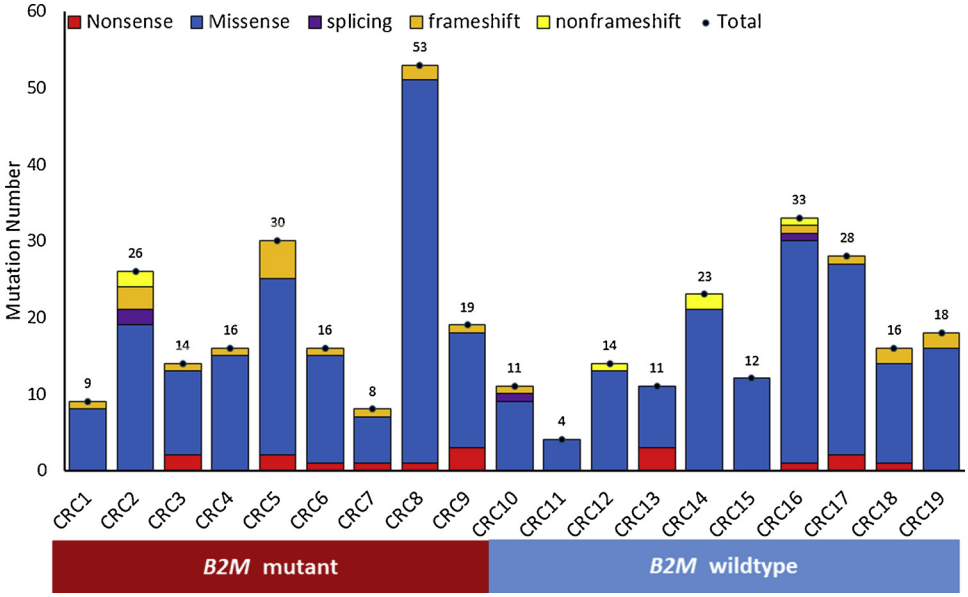

Fig. 1. The mutational feature of 19 colorectal cancers identified by a targeted deep sequencing with 119 genes. Number of somatic mutations of 19 CRC genomes are shown with respect to the mutation types as well as the *B2M* mutation status.

Table 2
Non-silent somatic mutations identified in the 19 colorectal cancers.

Gene	Case	Exonic function	cDNA change	Amino acid	Detection method*
B2M	CRC1	Frameshift	c.43_44delCT	p.L15fs	S, T
	CRC2	Frameshift	c.43_44delCT	p.L15fs	S, T
		Splicing	c.67 + 2T > C		S, T
	CRC3	Frameshift	c.43_44delCT	p.L15fs	S, T
	CRC4	Frameshift	c.43_44delCT	p.L15fs	S, T
	CRC5	Frameshift	c.16delG	p.A6fs	S, T
	CRC6	substitution	c.3 G > A	p.M1?	S, T
		Frameshift	c.43_44delCT	p.L15fs	S, T
	CRC7	Frameshift	c.43_44delCT	p.L15fs	S, T
	CRC8	Frameshift	c.43_44delCT	p.A6fs	S, T
	CRC9	Frameshift	c.43_44delCT	p.L15fs	S, T
		Frameshift	c.42_45delTCTT	p.S16fs	T
APC	CRC9	Nonsense	c. 1636C > T	p.R546X	T
	CRC12	Missense	c. 6610C > T	p.P2204S	T
	CRC13	Nonsense	c. 940C > T	p.R314X	T
		Nonsense	c. 4600 G > T	p.E1534X	T
	CRC15	Missense	c.5159 A > C	p.H1720P	T
	CRC17	Missense	c.5159 A > C	p.H1720P	T
	CRC18	Frameshift	c.4607dupA	p.E1536fs	T
TP53	CRC3	Missense	c.302 A > G	p.H101R	T
	CRC4	Missense	c.421C > T	p.R141C	T
	CRC5	Missense	c.416 A > G	p.E139G	T
		Missense	c.431C > T	p.A144V	T
	CRC9	Missense	c.124 A > G	p.R42G	T
	CRC11	Missense	c.347 G > A	p.R116Q	T
	CRC13	Missense	c.334C > A	p.G112S	T
PIK3CA	CRC3	Missense	c.3140 A > G	p.H1047R	T
		Missense	c.2176 G > A	p.E726K	T
	CRC8	Missense	c.1258 T > C	p.C420R	T
		Missense	c.3193C > T	p.H1065Y	T
	CRC9	Missense	c.1345C > T	p.P449S	T
		Missense	c.241 G > A	p.E81K	T
	CRC16	Missense	c.1367 T > G	p.L456R	T
	CRC17	Missense	c.649C > T	p.P217S	T
	CRC18	Missense	c.278 G > A	p.R93Q	T
		Missense	c.1637 A > G	p.Q546R	T
ERBB2	CRC5	Missense	c.649C > T	p.R217C	T
	CRC8	Missense	c.650 G > A	p.R217H	T
	CRC9	Missense	c.2033 G > A	p.R678Q	T
	CRC19	Missense	c.2264 T > C	p.L755S	T
		Missense	c.2033 G > A	p.R678Q	T
FGFR1	CRC3	Missense	c.359 G > A	p.R120H	T
	CRC4	Missense	c.830C > T	p.P277L	T
	CRC5	Missense	c.1450C > A	p.L484M	T
	CRC8	Missense	c.1610C > T	p.A537V	T
TSC2	CRC2	Missense	c.1319 T > C	p.F440S	T
	CRC3	Missense	c.212 G > A	p.S71N	T
	CRC5	Missense	c.1147 G > A	p.A383T	T
	CRC8	Missense	c.2062C > A	p.L688M	T
ARID1A	CRC2	Missense	c.1781 A > G	p.Q594R	T
	CRC8	Missense	c.2988 G > T	p.K996N	T
ERBB4	CRC6	Missense	c.3347C > T	p.P1116L	T
	CRC8	Missense	c.2693C > G	p.T898S	T
ATM	CRC2	Missense	c.6491 A > G	p.E2164G	T
	CRC4	Missense	c.4610 A > G	p.Q1537R	T
	CRC5	Missense	c.5012 T > A	p.V1671D	T
	CRC17	Missense	c.4514C > T	p.A1505V	T
IGF1R	CRC1	Missense	c.709 G > T	p.G237C	T
	CRC5	Missense	c.2491 G > A	p.A831T	T
	CRC6	Missense	c.3578C > T	p.S1193L	T
	CRC13	Missense	c.4012 G > A	p.A1338T	T
	CRC16	Missense	c.3736C > T	p.R1246C	T
FBXW7	CRC2	Missense	c.257C > T	p.S86L	T
	CRC8	Missense	c.1159C > T	p.R387C	T
	CRC19	Missense	c.1159C > T	p.R387C	T
PTEN	CRC17	Nonsense	c.740 T > A	p.L247X	T
	CRC18	Frameshift	c.795dupA	p.L265fs	T
BRAF	CRC5	Missense	c. 1799 T > A	p.V600E	T
	CRC18	Missense	c.1447 A > G	p.K483E	T
KDR	CRC8	Missense	c.2306 T > C	p.V769A	T
	CRC10	Missense	c.2836C > T	p.R946C	T
KRAS	CRC1	Missense	c.35 G > A	p.G12D	T
	CRC10	Missense	c.436 G > C	p.A146P	T
SMAD4	CRC4	Missense	c.1219 G > A	p.V407I	T
	CRC8	Missense	c. 396 C > A	p.H132Q	T

* S: Sanger sequencing, T: targeted NGS sequencing.

the *B2M* gene resides in the CRCs.

3.4. Immunohistochemical analysis

Because B2M is essential for antigen presentation and thus *B2M* inactivation is known to play a role in the resistance of ICB treatment, we attempted to find whether there would be any difference of cytotoxic CD8 + T cell numbers in the cancer tissues between *B2M*-mutated and *B2M*-wild-type CRCs. We identified 233–2637 CD8 + T cell at 10 HPFs (average: 893) in 19 CRCs (Supplementary Table 5). However, there was no significant difference in the CD8 + T cell numbers between *B2M*-mutated and wild-type cases ($P > 0.05$). The 9 *B2M*-mutated MSU CRCs were either MLH1-negative (n = 7) or MSH2-negative (n = 2) while the 10 B2M-wild-type MSU CRCs were either MLH1-negative (n = 8) or MSH2-negative (n = 1).

4. Discussion

The aim of the present study was twofold. First, we attempted to find the mutational distribution of *B2M* gene across diverse benign and malignant tumors. Of the malignant tumors, *B2M* mutations in the hotspot were detected only in MSU CRCs and hematopoietic tumors. In benign tumors, there was no *B2M* mutation detected. We identified a novel frameshift mutation (c.16delG) and a novel substitution mutation in 5′-untranslated region (c.-4C > T) as well as previously known frameshift mutations (c.del43-44CT, c.42_45delTCTT) and a splicing site mutation (c.67 + 2T > C). Second, we attempted to address genetic features of *B2M*-mutated MSU CRCs using a targeted NGS panel and found that the mutated cases exhibited a relatively larger driver mutation load and tended to harbor more *TP53* mutations and less *APC* mutations than *B2M*-wild-type MSU CRCs.

High incidence of frameshift mutations (80%, Table 1 and Supplementary Table 4) and preferred tissue distributions (CRC and hematopoietic tumors) in our study are in agreement with the COSMIC database (http://cancer.sanger.ac.uk/cosmic/), which currently catalogues 248 cancers with *B2M* somatic non-silent mutations that consist of mainly inactivation-type mutations (57% as frameshift and nonsense mutations) in CRCs and hematopoietic tumors. In the present study, we discovered a characteristic of the CRCs with *B2M* mutations, i.e., MSU phenotype, that had not been reported in previous studies [21–23]. Since MSU CRC is a main target for ICB therapies [5,6], our data may provide valuable information for assessing resistance to ICB therapies in MSU CRCs. Mutational abundance and *TP53* mutation preference in *B2M*-mutated MSU CRCs might pose a hypothesis that *B2M* mutation could possibly shape the cancer genomes. For this, further functional studies, as well as mutation studies in a larger MSU CRC cohort, will be needed.

Cancers with MSU phenotype by dMMR share common features irrespective of tissue origins (colon, stomach and uterus) such as high incidence of somatic mutations in mono- or dinucleotide repeats and low incidence of CNA as well as a favorable response to ICB [5,6,24]. Our and COSMIC data, however, suggest that MSU phenotype does not directly seem to be related to *B2M* mutation status. For instance, MSU stomach cancers in our data (Table 1) and endometrial cancers in the COSMIC data displayed much lower *B2M* mutation incidences than MSU CRCs. Also, the hotspot *B2M* frameshift mutations did not occur at mono- or dinucleotide repeats (Table 1), suggesting that the high

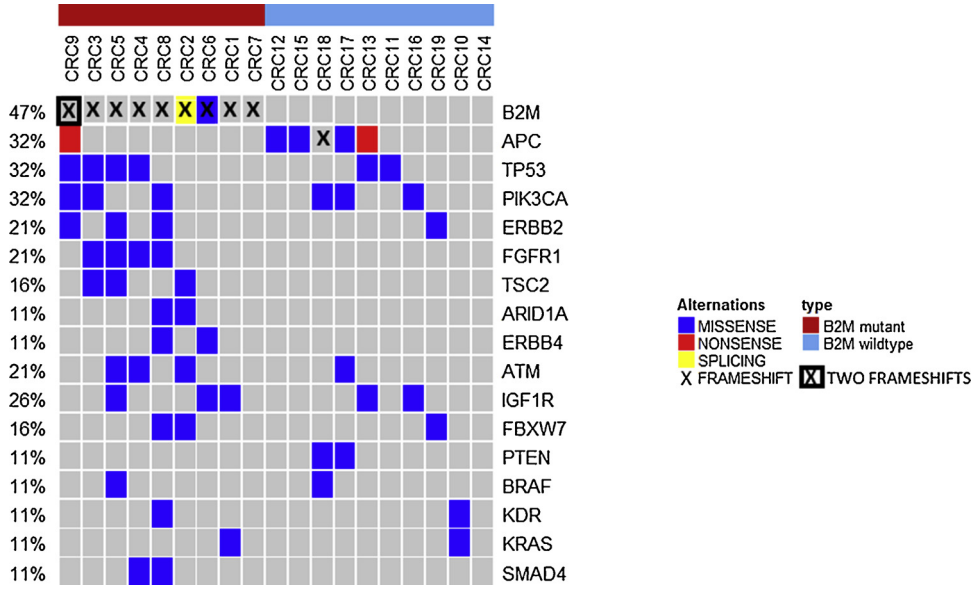

Fig. 2. Driver mutations in *B2M*-mutated and *B2M*-wild-type colorectal cancers. Cancer-related driver genes are listed for each sample with the frequencies in *B2M*-mutated and *B2M*-wild-type colorectal cancers.

incidence of the *B2M* mutation might not come from CRC or MSU alone.

CRCs are frequently resistant to the ICB treatment compared with other tumors, but better clinical responses just in the CRCs with MSU. However, many of the CRCs with MSU still do not respond well to the ICB [5]. The results in our study indicated that all of the *B2M* mutations in CRCs were found only in MSU cases, but not in MSS cases. Our data suggest that *B2M* mutation is one of the mechanisms for resistance to ICB treatment in MSU CRC, but may not be a mechanism for the resistance in MSS CRC.

To identify biological significances of *B2M* mutations, we measured the CD8 + T cells in MSU CRCs, but found no significant difference in the cell numbers between *B2M*-mutated and non-mutated CRCs (without prior ICB therapies). This result is in agreement with an earlier report that the presence of an adaptive immune signature is able to predict responders for ICB therapy in early on-treatment biopsies, but not in pre-treatment biopsies [25]. It could be that tissues in our study were not treated with immunotherapy and therefore the immune response had not yet been triggered. In addition, we did not find any association of clincopathologic parameters with *B2M* mutations in the CRCs. Together the data suggest that *B2M* mutation in CRCs might not influence on biological behaviors of CRCs without ICB treatment, but on those with the treatment.

Progressive accumulation of *B2M* alterations (mono-allelic to bi-allelic alterations) has been observed during and after the ICB therapies [5,8,11,14]. In the present study, we found that three cases (CRC2, CRC6 and CRC9 without prior ICB therapies) showed bi-allelic *B2M* alterations (Supplementary Table 4), suggesting that a careful evaluation is needed for using *B2M* alterations as a biomarker for ICB therapies. The second allelic alterations in our study are either a low-level frameshift mutation or a substitution mutation at the start codon or a splicing site mutation, functional consequences of which remain undetermined.

In summary, we report here the genetic alterations of ICB treatment-related *B2M* in a wide array of benign and malignant tumors and the genomic structures of *B2M*-mutated CRCs, which may provide useful information for understanding *B2M*-related immune alterations in cancers. Our results showed that MSU CRCs harbored *B2M* mutations more frequently and that *B2M*-mutated MSU CRCs harbored more driver mutations than *B2M*-wild-type MSU CRCs. Also, our study suggests that bi-allelic *B2M* alteration may not be uncommon and that its potential clinical implications should be further considered. Practically, when applying ICB therapies for CRC patients, clinicians should be aware that *B2M* mutation is common in MSU CRC, which could lead to resistance to the therapies.

Conflict of interest statement

All of the authors declare the absence of any conflict of interest.

Acknowledgements

This study was supported by a grant from National Research Foundation of Korea (2012R1A5A2047939).

Appendix A. Supplementary data

Supplementary data associated with this article can be found, in the online version, at https://doi.org/10.1016/j.prp.2018.11.014.

References

[1] S.L. Topalian, J.M. Taube, R.A. Anders, D.M. Pardoll, Mechanism-driven biomarkers to guide immune checkpoint blockade in cancer therapy, Nat. Rev. Cancer 16 (2016) 275–287.
[2] K.M. Mahoney, P.D. Rennert, G.J. Freeman, Combination cancer immunotherapy and new immunomodulatory targets, Nat. Rev. Drug Discov. 14 (2015) 561–584.
[3] M.K. Callahan, M.A. Postow, J.D. Wolchok, Targeting T cell co-receptors for cancer therapy, Immunity 44 (2016) 1069–1078.
[4] M.W. Teng, R. Khanna, M.J. Smyth, Checkpoint immunotherapy: picking a winner, Cancer Discov. 6 (2016) 818–820.
[5] D.T. Le, J.N. Durham, K.N. Smith, H. Wang, B.R. Bartlett, L.K. Aulakh, et al., Mismatch repair deficiency predicts response of solid tumors to PD-1 blockade, Science 357 (2017) 409–413.
[6] O. Hamid, C. Robert, A. Daud, F.S. Hodi, W.J. Hwu, R. Kefford, et al., Safety and tumor responses with lambrolizumab (anti-PD-1) in melanoma, N. Engl. J. Med. 369 (2013) 134–144.
[7] D. Pardoll, Cancer and the Immune System: basic concepts and targets for intervention, Semin. Oncol. 42 (2015) 523–538.
[8] J.M. Zaretsky, A. Garcia-Diaz, D.S. Shin, H. Escuin-Ordinas, W. Hugo, S. Hu-Lieskovan, et al., Mutations associated with acquired resistance to PD-1 blockade in melanoma, N. Engl. J. Med. 375 (2016) 819–829.
[9] K. Kataoka, Y. Shiraishi, Y. Takeda, S. Sakata, M. Matsumoto, S. Nagano, et al., Aberrant PD-L1 expression through 3'-UTR disruption in multiple cancers, Nature 534 (2016) 402–406.
[10] N. Shastri, S. Cardinaud, S.R. Schwab, T. Serwold, J. Kunisawa, All the peptides that fit: the beginning, the middle, and the end of the MHC class I antigen-processing pathway, Immunol. Rev. 207 (2005) 31–41.
[11] S. Gettinger, J. Choi, K. Hastings, A. Truini, I. Datar, R. Sowell, et al., Impaired HLA

class I antigen processing and presentation as a mechanism of acquired resistance to immune checkpoint inhibitors in lung cancer, Cancer Discov. 7 (2017) 1420–1435.
[12] N.P. Restifo, F.M. Marincola, Y. Kawakami, J. Taubenberger, J.R. Yannelli, S.A. Rosenberg, Loss of functional beta 2-microglobulin in metastatic melanomas from five patients receiving immunotherapy, J. Natl. Cancer Inst. 88 (1996) 100–108.
[13] C.M. D'Urso, Z.G. Wang, Y. Cao, R. Tatake, R.A. Zeff, S. Ferrone, Lack of HLA class I antigen expression by cultured melanoma cells FO-1 due to a defect in B2m gene expression, J. Clin. Invest. 87 (1991) 284–292.
[14] A. Sucker, F. Zhao, B. Real, C. Heeke, N. Bielefeld, S. Maβen, et al., Genetic evolution of T-cell resistance in the course of melanoma progression, Clin. Cancer Res. 20 (2014) 6593–6604.
[15] V.H. Koelzer, K. Baker, D. Kassahn, D. Baumhoer, I. Zlobec, Prognostic impact of β-2-microglobulin expression in colorectal cancers stratified by mismatch repair status, J. Clin. Pathol. 65 (2012) 996–1002.
[16] M.R. Kang, M.S. Kim, J.E. Oh, Y.R. Kim, S.Y. Song, S.S. Kim, et al., Frameshift mutations of autophagy-related genes ATG2B, ATG5, ATG9B and ATG12 in gastric and colorectal cancers with microsatellite instability, J. Pathol. 217 (2009) 702–706.
[17] S.H. Jung, S. Shin, M.S. Kim, I.P. Baek, J.Y. Lee, S.H. Lee, et al., Genetic progression of high grade prostatic intraepithelial neoplasia to prostate cancer, Eur. Urol. 69 (2016) 823–830.
[18] K. Cibulskis, M.S. Lawrence, S.L. Carter, A. Sivachenko, D. Jaffe, C. Sougnez, et al., Sensitive detection of somatic point mutations in impure and heterogeneous cancer samples, Nat. Biotechnol. 31 (2013) 213–219.
[19] M.A. DePristo, E. Banks, R. Poplin, K.V. Garimella, J.R. Maguire, C. Hartl, et al., A framework for variation discovery and genotyping using next-generation DNA sequencing data, Nat. Genet. 43 (2011) 491–498.
[20] K. Wang, M. Li, H. Hakonarson, ANNOVAR: functional annotation of genetic variants from high-throughput sequencing data, Nucleic Acids Res. 38 (2010) e164.
[21] M. Giannakis, X.J. Mu, S.A. Shukla, Z.R. Qian, O. Cohen, R. Nishihara, et al., Genomic correlates of immune-cell infiltrates in colorectal carcinoma, Cell Rep. 15 (2016) 857–865.
[22] D. Mouradov, C. Sloggett, R.N. Jorissen, C.G. Love, S. Li, A.W. Burgess, D. Arango, et al., Colorectal cancer cell lines are representative models of the main molecular subtypes of primary cancer, Cancer Res. 74 (2014) 3238–3247.
[23] Cancer Genome Atlas Network, Comprehensive molecular characterization of human colon and rectal cancer, Nature 487 (2012) 330–337.
[24] K. Imai, H. Yamamoto, Carcinogenesis and microsatellite instability: the interrelationship between genetics and epigenetics, Carcinogenesis 29 (2008) 673–680.
[25] P.L. Chen, W. Roh, A. Reuben, Z.A. Cooper, C.N. Spencer, P.A. Prieto, et al., Analysis of immune signatures in longitudinal tumor samples yields insight into biomarkers of response and mechanisms of resistance to immune checkpoint blockade, Cancer Discov. 6 (2016) 827–837.